# Fiber Bragg Grating-Based Large Nonblocking Multiwavelength Cross-Connects

Yung-Kuang Chen, *Member, IEEE, Member, OSA,* and Chien-Chung Lee

***Abstract*— Multiwavelength cross-connects (WXC's) will play a key role to provide more reconfiguration flexibility and network survivability in wavelength division multiplexing (WDM) transport networks. In this paper, we utilize three different fiber Bragg grating (FBG)-based $P$-type, $S$-type, and $N$-type building blocks with optical circulators and related control devices for constructing large rearrangeably *nonblocking* $N \times N$ WXC's. The $P$-type building block is composed of certain *"parallel"* FBG-element chains placed between the control devices of two large mechanical optical switches (OSW's). The $S$-type building block consists of a *"series"* of FBG elements and the control device of $2 \times 2$ OSW's. The nonswitched $N$-type building block includes a *"series"* of FBG elements with appropriate stepping motor or PZT control devices. All FBG elements, each with central wavelength corresponding to equally or unequally spaced WDM channel wavelengths, with high-reflectivity are required. Large $N \times N$ WXC structures, with minimum number of required constitutive elements, based on a three-stage Clos network are then constructed. We investigate their relevant characteristics, compare the required constitutive elements, and estimate the dimension limits for these WXC architectures. Other related issues such as capacity expansion, wavelength channel spacing, and multiwavelength amplification are also addressed.**

***Index Terms*— Fiber Bragg grating, optical cross-connect (OXC), optical network, wavelength cross-connect (WXC), wavelength division multiplexing (WDM).**

## I. Introduction

THE wavelength division multiplexing (WDM) technique combining with erbium-doped fiber amplifiers (EDFA's) has shown its capability to cost-effectively, gracefully upgrade the capacity of embedded long-distance transmission systems [1], [2]. The extensive deployments of such WDM amplified point-to-point transmission systems and/or SONET/SDH ring networks open the perspective of efficiently performing network functions in the optical domain. Thus, new optical elements are required to provide additional facilities for WDM signals locally transmitting/extraction (i.e., the add–drop operation), for signal routing and network (re)configuration (i.e., the cross-connect operation) in such WDM transport networks. Optical wavelength cross-connect (WXC), one of the new network elements, will play a key role in multiwavelength WDM networks [3]–[5]. The importance of the WXC's is that they allow the optical network to be reconfigured on a wavelength-by-wavelength basis to optimize traffic, congestion, network growth, and to enhance network survivability.

Although many experimental implementations of WXC's exist today, it is possible to make a distinction between two major classes: wavelength-routing and wavelength-translating WXC's [3]. Wavelength routing is achieved by implementing some form of wavelength-selective elements at the nodes of the fiber network. Fixed wavelength routing WXC would most likely use WDM multiplexers in a back-to-back configuration to allow interchange of wavelengths between input and output fibers in a prearranged pattern. This configuration as shown in Fig. 1(a) has been called a *fixed* WDM cross-connect, and in its simplest form does not have any automated rearrangeability. The rearrangeability is introduced by adding space division (SD) switches, as shown in Fig. 1(b). Using such rearrangeable WDM WXC's, each wavelength on any input fiber can be interconnected to any output fiber providing that output fiber is not already using that wavelength. The total cross-connect bandwidth is proportional to $N \cdot m \cdot B$ where $N$ is the number of input fibers, $m$ is the number of wavelengths per fiber, and $B$ is the bit rate per wavelength channel. Different space-division switch technologies based on such as waveguide directional couplers [6], semiconductor optical amplifiers (SOA's) [7], low-gain EDFA's [8], and arrayed-waveguide grating (AWG) multiplexes [9] have been demonstrated. The basic operation for both of the above wavelength-routing WXC's is that they select wavelengths and rearrange them in the spatial domain. The second category of WXC has recently been defined to allow cross-connect in the wavelength domain as well as the space domain, and has been called a wavelength-translating (or -interchanging) cross-connect, one form of which is shown in Fig. 1(c). However, various wavelength conversion [10], [11] and wavelength interchange techniques [5] are inevitable. The fiber Bragg grating-based WXC's described in this paper belong to the wavelength-routing category.

From the viewpoint of blocking performance, WXC's can be classified into nonblocking and blocking networks [4]. Nonblocking networks can be further divided into strictly nonblocking [12] and rearrangeably nonblocking [12] networks. If a WXC is strictly nonblocking, any idle input wavelength channel on any input fiber can always be connected to any unused output wavelength on any output fiber without disturbing any existing wavelength connections [12]. If it is rearrangeably nonblocking, any idle input wavelength channel on any input fiber can always be connected to any unused output wavelength channel on any output fiber by

Manuscript received January 20, 1998; revised June 5, 1998.

Y.-K. Chen is with the Institute of Electro-Optical Engineering, National Sun Yat-Sen University, Kaohsiung 804 Taiwan.

C.-C. Lee is with the Outside-Plant Division, Chung-Hwa Telecommunication Laboratories, Yang-Mei 326 Taiwan. He is also with the Institute of Electro-Optical Engineering, National Chiao-Tung University, Hsinchu, Taiwan.

Publisher Item Identifier S 0733-8724(98)07405-2.

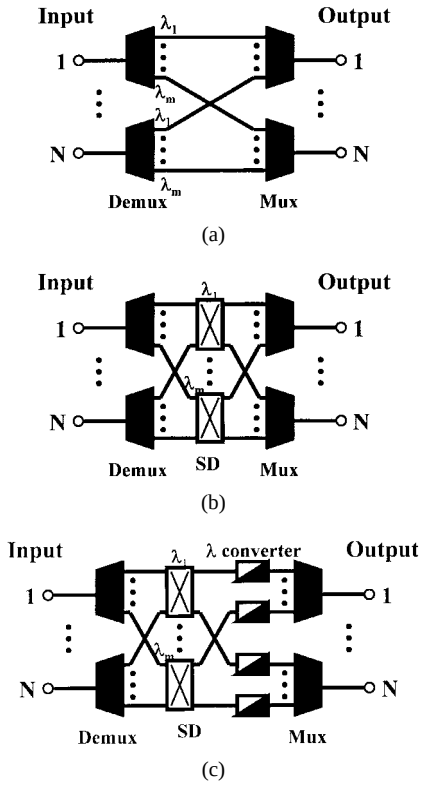


Fig. 1. Schematic diagrams of three-category WXC's with $N$ input–output port pairs and $m$ wavelengths per fiber: (a) a fixed WXC, (b) a rearrangeable WXC using space division (SD) switches, and (c) a wavelength-translating WXC using wavelength converters with fixed-wavelength outputs and variable inputs.

rerouting the existing wavelength connections if necessary [13]. However, the architecture for constructing a strictly nonblocking WXC is always more complicated with many required wavelength converters and/or space-division switches than a rearrangeably nonblocking one [4], [6], [8], thus more expensive to be used. Since WXC is mainly used for 1) efficient network utilization, 2) network restortation, and 3) customer control and management, fast switching is generally not required. Therefore, a WXC is a nonblocking "slow" switch network with a connection duration of hours or months, and cross-connects much higher rate signals. The rearrangeably nonblocking WXC's can satisfy most network applications. The objective of this paper is to investigate the rearrangeably nonblocking WXC's.

Fiber Bragg grating (FBG) filter is a periodic perturbation of the refractive index along the fiber length, which is formed by exposure of the core to an intense optical interference pattern. The formation of permanent gratings in an optical fiber was first demonstrated by Hill *et al.* in 1978 [14]. Meltz *et al.* [15] showed that the ultraviolet radiation at 248 nm could be used to form gratings that would reflect any wavelength by illuminating the fiber through the side of the cladding with two intersecting beams of ultraviolet (UV) laser lights. Advantages of FBG's over competing technologies include all-fiber geometry, low insertion loss, low back-reflection, and potentially low cost. But the most distinguishing feature of FBG's is the flexibility they offer for achieving desired sharp spectral characteristics. They are now commercially available

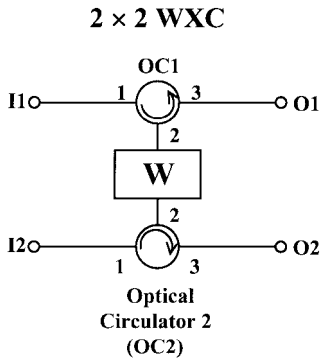


Fig. 2. Schematic diagram of the proposed FBG-based 2 × 2 WXC. OC: three-port optical circulator. There are two input ports (I1 and I2) and two output ports (O1 and O2) for each 2 × 2 WXC. "**W**": the basic building block of proposed WXC.

and they have found important applications in a variety of lightwave applications [16], [17].

Recently, a wavelength selective add–drop multiplexer (ADM), another network element with locally transmitting/extraction functions for WDM transport network, comprising the reflective FBG's and optical switches was proposed [18] and system demonstrated [19]. We have successfully reformed the FBG-based ADM into a dynamically wavelength selective 2 × 2 WXC [20]. The demonstration and system performance of this FBG-based WXC have shown its capability to provide more reconfiguration flexibility for WDM networks. However, this FBG-based 2 × 2 WXC with two input/output ports has limited applications in WDM transport networks. With the motivation of investigating large nonblocking $N \times N$ WXC's that have large input/output dimension with multiple wavelength channels, this paper proposes a class of FBG-based basic building blocks for construction of large $N \times N$ WXC's for network applications. The relevant characteristics and required constitutive elements are investigated and compared. Some key issues associated with the FBG-based WXC's are also addressed.

The rest of the paper is organized as follows. In Section II, three kinds of FBG-based basic building blocks for constructing large $N \times N$ WXC's are proposed and their operation principles are described. The large $N \times N$ WXC architectures based on a Clos network using these building blocks are also presented. Section III describes their relevant characteristics, and compares the required constitutive elements. WXC dimension limits for different architectures are presented in Section IV. Other issues such as capacity expansion, wavelength channel spacing, and multiwavelength amplification are discussed in Section V. Section VI summarizes the paper and presents our conclusions.

## II. Basic Building Blocks and Architectures for FBG-Based WXC's

Fig. 2 shows the schematic diagram of an FBG-based 2 × 2 WXC. There are two input ports (I1 and I2) and two output ports (O1 and O2), thus the WXC dimension, $N$, equals to 2. The 2 × 2 WXC is composed of two three-port optical circulators (OC's) and the basic building block "**W**." Three

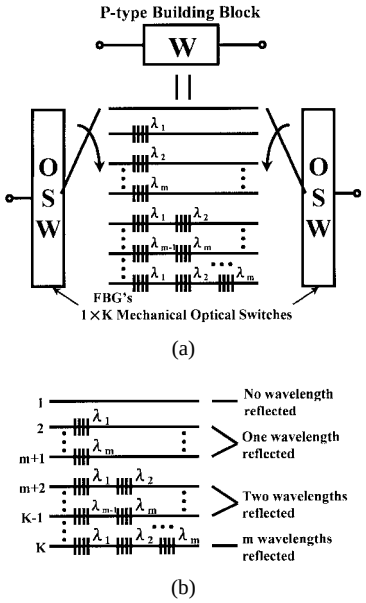


Fig. 3. The (a) schematic diagram of the "*parallel*" $P$-type building block "**W**" and (b) illustration of its operating principle.

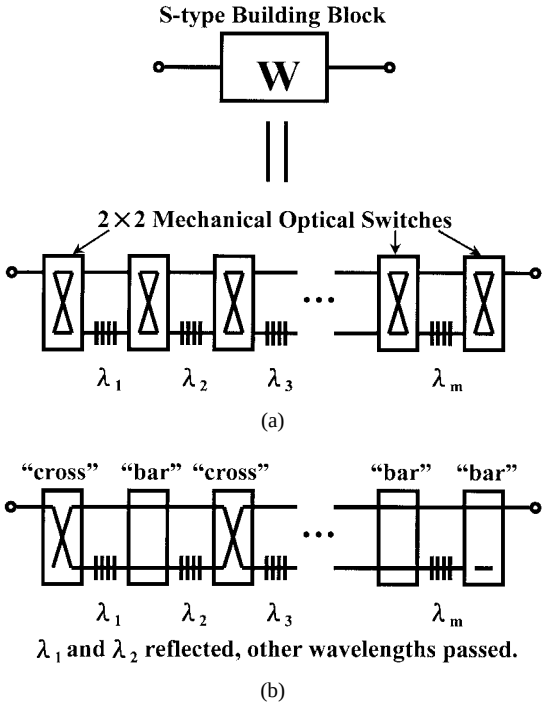


Fig. 4. The (a) schematic diagram of the "*series*" $S$-type building block "**W**" and (b) illustration of its operating principle.

kinds of the $P$-, $S$-, and $N$-type building blocks are proposed. The $P$-type block, as shown in Fig. 3(a), is named due to certain "*parallel*" FBG chains placed between two $1 \times K$ mechanical optical switches (OSW's). Each central reflective wavelength $\lambda_i$ of the FBG$_i$ is designed to match the used WDM channel wavelength. The FWHM (i.e., 3-dB passband width) of each FBG should be large enough to cover the corresponding channel signal with high reflectivity and low out-of-band transmission loss. Switching the OSW-pair to proper FBG$_i$ position, the desired channel signal $\lambda_i$ will be reflected by the connected FBG$_i$, as shown in Fig. 3(b), then leaving from the port 3 of the OC1 in Fig. 2, and continuing its forward propagation (here, termed as the *passed-through* channel) in the same fiber link. In the mean time, other channel signals can be spatially passed through the FBG chain (here, termed as the *cross-connected* channels) to another fiber link. When two or more FBG's in a single cascading chain, as shown in Fig. 3(b), are properly arranged between the $1 \times K$ OSW's, multiple channel cross-connections can be realized. Furthermore, the first optical path without any FBG's is for cross-connecting all wavelengths, and the last $K$th optical path with $m$ pieces of different FBG's is for passing through all channel wavelengths. The simple $1 \times K$ OSW can be used for this function with switching time of about 0.3 ms. For rearrangeably nonblocking operation, the OSW size, $K$, and the number of required $1 \times K$ OSW's, $U$, for a $P$-type $2 \times 2$ WXC is $K = 2^m$, and $U = 2$, respectively. The total number, $Q$, of required FBG's for a $P$-type $2 \times 2$ WXC is

$$Q = \binom{m}{0} \cdot 0 + \binom{m}{1} \cdot 1 + \binom{m}{2} \cdot 2 + \cdots + \binom{m}{m} \cdot m = 0 + m + \frac{m(m-1)}{1!} + \frac{m(m-1)(m-2)}{2!} + \cdots + m. \quad (1)$$

The $m$ is the number of WDM channel wavelengths used per fiber. Therefore, the larger WDM channels $m$, the larger OSW size $K$ and the more increased total grating number $Q$. The feasibility of this $P$-type $2 \times 2$ WXC with negligible bit-error-rate (BER) power penalty has been demonstrated in a $3 \times 2.5$ Gb/s WDM 100-km system experiment [20].

Fig. 4(a) shows the $S$-type building block, in which a "*series*" of FBG elements and $2 \times 2$ OSW's are used with each FBG inserted between two $2 \times 2$ OSW's. Each $2 \times 2$ OSW has one of the "*cross*" and "*bar*" operation states at one time. Switching two $2 \times 2$ OSW's, one in front of and one after the FBG element, to the "*cross*" state, the passed-through channel signal will be reflected by the connected FBG element, then leaving from the port 3 of the OC1 at the same fiber link as shown in Fig. 2. In the mean time, other crossed-connected channel signals can be spatially passed through the FBG chain to another fiber link. When two or more $2 \times 2$ OSW's are properly arranged in the $S$-type building block, multiple channel cross-connections can then be realized. Fig. 4(b) illustrates that the wavelengths $\lambda_1$ and $\lambda_2$ are simultaneously reflected and thus passed-through the $2 \times 2$ WXC when the first and the third OSW's are in the "*cross*" states and other OSW's are in the "*bar*" states. For rearrangeably nonblocking operation, the number of required $2 \times 2$ OSW's, $U$, and total number of required FBG's, $Q$, of an $S$-type $2 \times 2$ WXC is $U = m+1$ and $Q = m$, respectively. A $2 \times 2$ ADM comprising chirped FBG's in an $S$-type-like block for dispersion compensating and reconfigurable ADM multiplexing operation with error-free performance has been demonstrated in a $4 \times 10$ Gb/s WDM 50-km system experiment [19]. This reveals the feasibility of the proposed $S$-type building block.

Fig. 5(a) shows the nonswitched $N$-type basic building block, in which a "*series*" of FBG's with appropriate control

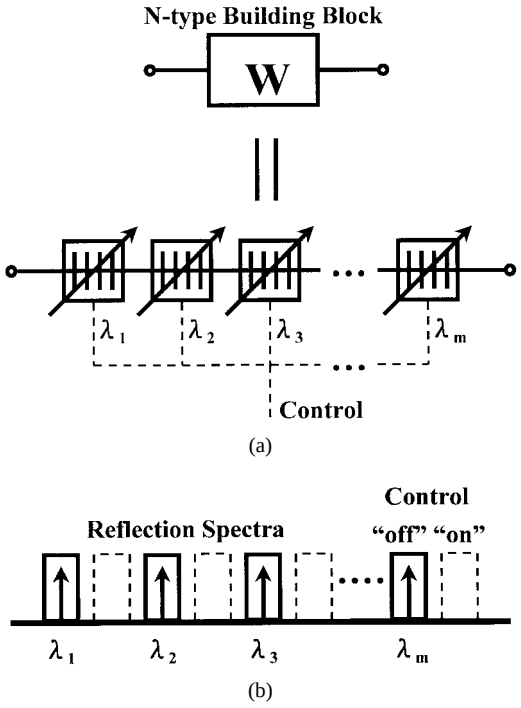


Fig. 5. The (a) schematic diagram of the "*nonswitched*" $N$-type building block "**W**" and (b) illustration of its operating principle.

devices are used but with no more OSW's. The central wavelength-shift control of each FBG in this $N$-type WXC can be achieved by using tensile stress or compressive stress on the FBG. Strain tuning yields a Bragg wavelength change of approximately 1.2 nm/millistrain in the 1.55-$\mu$m regime [21]. Bragg grating wavelength tuning by tensile stress is limited by fiber strength, and the maximum tuning to a 10-nm regime is limited. The fiber strength limitations associated with tensile stress are relieved when compressive stress is implemented, because silica is 23 times stronger under compression than under tension, thus a tuning range of $>$32 nm has been demonstrated [21]. In Ball and Moreys' experiments [21], a high-resolution stepping motor was used to compress the fiber, which was confined within the precision-ground ceramic ferrules. The 400-step/revolution micropositioner could be driven with 10 000 microstep/revolution with a $\pm$1-microstep resolution. This resulted in a linear translation resolution of $\pm$50 nm, a wavelength resolution of $\pm$2 pm, and a frequency resolution of $\pm$250 MHz. This Bragg wavelength tuning technique by compression stress is mechanically simple to implement, and thus can be used to control the Bragg wavelength tuning of each FBG in the proposed $N$-type building block.

The operating mechanism of the nonswitched $N$-type basic building block is illustrated in Fig. 5(b). Assume that all FBG's meet the International Telecommunication Union (ITU) WDM standardization with 200 GHz (about 1.6 nm) and with an FWHM bandwidth of 75 GHz (about 0.6 nm). By controlling the stepping motor to compress the FBG to make an increasingly (or decreasingly) change of the central wavelength to a 100-GHz shift, then the desired channel signals can be spatially cross-connected to another fiber link. Otherwise, the signal will be reflected by the un-compressed FBG. When

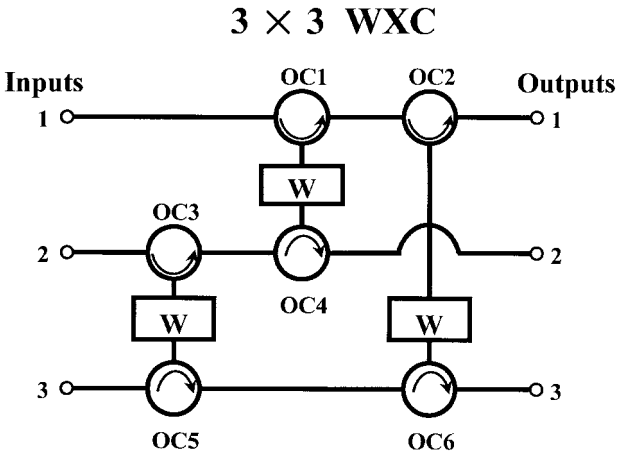


Fig. 6. The rearrangeably nonblocking 3 $\times$ 3 WXC constructed with optical circulators and the basic building blocks.

TABLE I
THE REQUIRED CONSTITUTIVE ELEMENTS FOR THREE PROPOSED FBG-BASED BASIC BUILDING BLOCKS

| *Block "W"* | *P-type* | *S-type* | *N-type* |
|---|---|---|---|
| *Control Device* | *1 × K OSW ($K = 2^m$)* | *2 × 2 OSW* | *Compressed FBGs by Step Motors or PZTs* |
| *Number of Control Devices* | *2* | *m + 1* | *m* |
| *FBG Number* | *m + m(m-1)/1! + m(m-1)(m-2)/2! +.....+ m* | *m* | *m* |

two or more FBG's are properly compressed by using separate stepping motors, then multiple channels' cross-connections can be realized as shown in Fig. 5(b). Besides the high-resolution stepping motors, the voltage-driven piezoelectrical transducer (PZT) devices seem an alternative for compression stress control of the FBG. After winding and adhering each FBG upon separate PZT rod, controlling the corresponding PZT supplying voltage(s) to compressed the FBG(s) to a 100-GHz shift, then the desired wavelength(s) can be cross-connected. On the other hand, the desired wavelength(s) will be reflected by the corresponding FBG(s), as shown in Fig. 5(b), when the PZT driving voltage(s) is (are) released. The PZT-controlled approach is now under study. Table I summaries the control devices and lists the required constitutive elements for these three FBG-based basic "**W**" building blocks. The above three FBG-based building-block-constructed 2 $\times$ 2 WXC's are all rearrangeably nonblocking devices.

Fig. 6 shows the rearrangeably nonblocking 3 $\times$ 3 WXC, consisting of three "**W**" building blocks and six three-port OC's. Any FBG-based $P$-type, $S$-type, or $N$-type building blocks could be placed in this 3 $\times$ 3 WXC to carry out cross-connected operations. The $N \times N$ WXC architectures based on three-stage Clos network are used to construct large dimension. The Clos network [12] is a three-stage network that offers a method of obtaining larger architectures by interconnecting several smaller nonblocking subnetworks. Each of the subnetworks could be broken down into its own

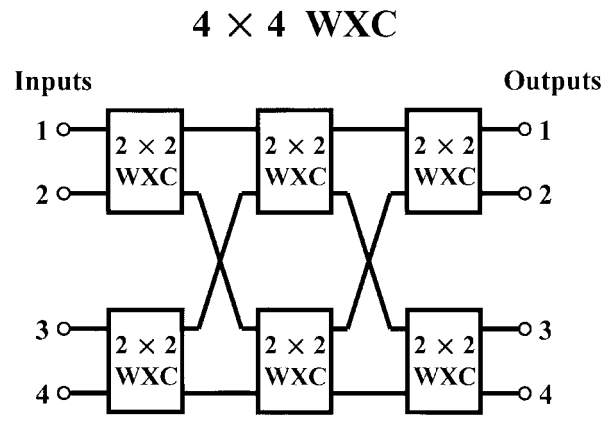


Fig. 7. The rearrangeably nonblocking 4 × 4 WXC constructed by using 2 × 2 WXC's in a three-stage Clos network architecture.

Clos network, with this procedure being applied recursively. For an overall $N \times N$ WXC, the first stage required $r$ subnetworks of dimension $i \times j$, where $r \times i = N$. The second stage requires $j$ subnetworks of dimension $r \times r$, and the third stage requires $r$ subnetworks of dimension $j \times i$. The Clos architecture is rearrangeably nonblocking if $j \geq i$.

Fig. 7 illustrates the rearrangeably nonblocking 4 × 4 WXC constructed by using 2 × 2 WXC's in a three-stage Clos network architecture, each stage with two 2 × 2 WXC's, thus a total of six required 2 × 2 WXC's. According to the nonbolcking criterion of Clos network, now $i = j = r = 2$, thus the WXC shown in Fig. 7 is rearrangeably nonblocking. Follow the construction criterion of three-stage Clos network, the rearrangeably nonblocking 8 × 8 WXC can be easily realized by using four 2 × 2 WXC's in the first stage, two 4 × 4 WXC's in the second stage, and four 2 × 2 WXC's in the third stage. Similarly, the three-staged rearrangeably nonblocking 9 × 9 WXC can be constructed with minimum number of building blocks of nine 3 × 3 WXC's, each stage with three 3 × 3 WXC's. According to the Clos network principle, the large rearrangeably nonblocking $N \times N$ WXC's with minimum number of building blocks can be realized for $N = 16, 32, 64$ or $27, 81$, etc. The number of required building blocks, hereinafter $W(n)$, for the rearrangeably nonblocking $N \times N$ WXC's is given below

$$W(n) = 2^n + 2 \cdot W(n-1), \quad \text{and} \quad W(1) = 1 \quad \text{for } N = 2^n. \quad \text{(2a)}$$

$$W(n) = 2 \cdot 3^n + 3 \cdot W(n-1), \quad \text{and} \quad W(1) = 3 \quad \text{for } N = 3^n \quad \text{(2b)}$$

where $W(n-1)$ is the previous value of $W(n)$; for instance, $W(1) = 1$, then $W(2) = 2^2 + 2 \cdot W(1) = 6$ for the case of 4 × 4 WXC with $N = 4$. The total number of OC's, $C_O$, required to implement an $N \times N$ WXC is two times of the number of total required building blocks "**W**," $W(n)$, namely, $C_O = 2 \cdot W(n)$, because two OC's are used in each building blocking "**W**." Fig. 8 shows the required building blocks "**W**" and the total number of OC's for the rearrangeably nonblocking $N \times N$ WXC's against network dimension.

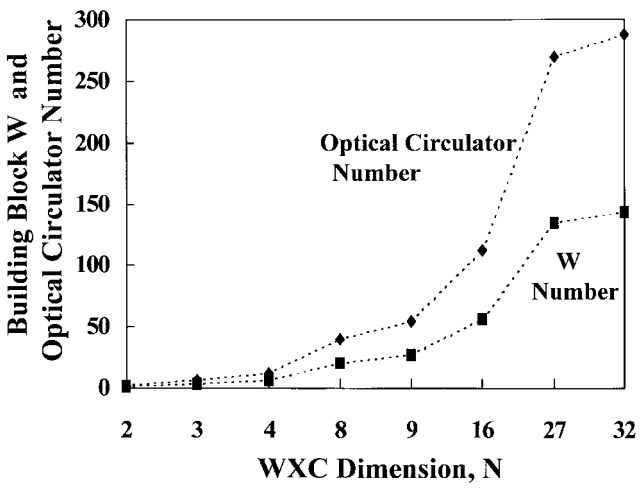


Fig. 8. The number of required building blocks "**W**" and the total number of optical circulators required to implement the rearrangeably nonblocking WXC's against network dimension $N$.

## III. Characteristic Comparison of WXC Architectures

The FBG-based large WXC's using different building blocks can be compared using several benchmarks. Each characteristic may single out a different architecture as being better than others for that characteristic. However, the overall optimal architecture for a specific application with specific WXC size depends on the relative weighting a designer would be different for every application. A brief description of several relevant WXC characteristics and the various characteristic comparisons versus WXC dimension for the $P$-type, $S$-type, and $N$-type WXC's follow.

### A. Descriptions of WXC Characteristics

The relevant FBG-based WXC characteristics include system attenuation, system signal-to-noise ratio (SNR), the numbers of FBG's, OC's, and control devices. The numbers of OC's, control devices, FBG's, and interconnected fibers that the given WDM signal path passes through determine the attenuation. Two important parameters exist here: the *worst case attenuation* for the highest loss path, and the *differential attenuation* between the highest loss path and the lowest loss path. Many times a high differential attenuation is more of a disadvantage than a high worst case attenuation. A high constant attenuation can be compensated for with the addition of EDFA's. A high differential attenuation adversely affects the optical receiver and can reduce the system SNR. The insufficient reflectivity of FBG and its peak-wavelength misalignment of the cross-connected and passed-through signals further affects system SNR. Various architectures require different numbers of FBG's, OC's, and control devices for the same WXC dimensionality. More these components mean high cost and difficult system interconnection.

In this section, characteristic comparisons versus WXC dimension are carried out for the $P$-type, $S$-type, and $N$-type WXC's. For high-capacity all-optical WDM networks, the WXC nodes should cross-connect $N$ sets of $m$-wavelength from $N$ input links to the same number of output links with operating bit-rate per channel, $B$, in the range from 2.5 to

TABLE II
THE SYSTEM PARAMETERS AND COMPONENT CHARACTERISTICS WITH THEIR TYPICAL VALUES USED FOR COMPARISON OF THE FBG-BASED $N \times N$ WXC's

| System and Component Parameters | Typical Values |
|---|---|
| WDM wavelengths per fiber, m: | 4, 8, 16 |
| Insertion loss of circulator | |
| Port 1 – 2: | 0.5 dB |
| Port 2 – 3: | 0.5 dB |
| Isolation loss of circulator: | >40 dB |
| Reflectivity of FBG: | > 99.7% |
| Insertion loss of FBG: | 0.05 dB |
| FWHM bandwidth: | 0.6 nm |
| Insertion loss of optical switch for 1 × K or 2 × 2 OSW's: (where K ≤ 256) | 0.9 dB |
| Return loss of all components: | > 65 dB |

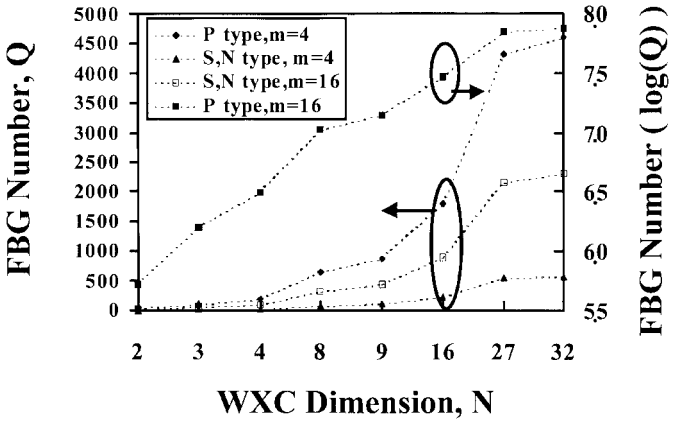


Fig. 9. The number of FBG elements, $Q$, required for the three FBG-based $N \times N$ WXC architectures. The parameter, $m$, is the WDM wavelengths per fiber.

10 Gb/s. In general, $m \approx 4-16$ and $N \approx 2-16$ [22], [23]. Table II lists the system parameters and component characteristics with their typical values used for comparison of the different FBG-based $N \times N$ WXC's.

### B. FBG Element Characteristics

The three-type WXC architectures require different numbers of FBG elements to implement an $N \times N$ WXC. The number of FBG elements, $Q$, required for each of the architectures for $N \times N$ is the number of required FBG elements for each building block, listed in Table I, multiplied by the required number $W(n)$ of building blocks described in (2), and is given below, which is strongly dependent on the number of operating wavelength, $m$, per fiber link, and for comparison is plotted in Fig. 9.

*1) P-Type $N \times N$ WXC:*

$$Q = \left[\binom{m}{0}\cdot 0 + \binom{m}{1}\cdot 1 + \binom{m}{2}\cdot 2 + \cdots + \binom{m}{m}\cdot m\right] \cdot W(n) \quad \text{for } N = 2^n \quad \text{and} \quad N = 3^n. \tag{3a}$$

*2) S-Type $N \times N$ WXC:*

$$Q = m \cdot W(n) \quad \text{for } N = 2^n \quad \text{and} \quad N = 3^n. \tag{3b}$$

*3) N-Type $N \times N$ WXC:*

$$Q = m \cdot W(n) \quad \text{for } N = 2^n \quad \text{and} \quad N = 3^n. \tag{3c}$$

Note that both $N$-type and $S$-type WXC's have the least number of FBG elements. The more number of WDM wavelengths per fiber used the larger number of required FBG elements. For instance, for a $4 \times 4$ WXC, the number of FBG elements is $Q = 24$ for $m = 4$, and $Q = 96$ for $m = 16$. However, The number of required FBG elements for the $P$-type $N \times N$ WXC are very large, which is drastically increased for large WXC dimension, especially for large number of WDM wavelengths used per fiber.

### C. Control Device Characteristics

The three-type WXC architectures also require different numbers of control devices to implement an $N \times N$ WXC. The control devices of each building blocking for the $P$-type, $S$-type, and $N$-type architectures are two $1 \times K$ OSW's, $m+1$ pieces of $2 \times 2$ OSW's, and $m$ pieces of high-resolution stepping motors or PZT devices. Consequently, the total number of control devices, $C$, required for each of the architectures is the number of control devices required for each building block, listed in Table I, multiplied by $W(n)$ described in (2), and is given below.

*1) P-Type $N \times N$ WXC:*

$$C = 2 \cdot W(n) \quad \text{for } N = 2^n \quad \text{and} \quad N = 3^n. \tag{4a}$$

*2) S-Type $N \times N$ WXC:*

$$C = (m+1) \cdot W(n) \quad \text{for } N = 2^n \quad \text{and} \quad N = 3^n. \tag{4b}$$

*3) N-Type $N \times N$ WXC:*

$$C = m \cdot W(n) \quad \text{for } N = 2^n \quad \text{and} \quad N = 3^n. \tag{4c}$$

The number of control devices is strongly dependent upon the number of WDM wavelengths per fiber link, and for comparison is illustrated in Fig. 10. Note that the $P$-type WXC's have the least number of control devices of $1 \times K$ OSW's. However, The number of required control devices for the $S$-type $N \times N$ WXC are very large, which is drastically increased for large WXC dimension, especially for large number of WDM wavelengths per fiber used. The number of control devices for the $N$-type WXC is about $W(n)$ less than that of the $S$-type WXC with same dimension.

### D. Attenuation Characteristics

The maximum system insertion loss, *SIL*, for an $N \times N$ WXC is dependent upon the number of OC's, FBG's, and associated OSW's that the signals traversing the worst-case path must travel. Assume that all FBG's has a high reflectivity of 99.7–99.9% with an out-of-band transmission insertion loss, $L_G$, of about 0.05 dB. Thus, the insertion loss for the reflected light can be neglected, due to the ultra-high FBG reflectivity. Each three-port OC has an insertion loss, $L_{\mathrm{OC}}$, either from

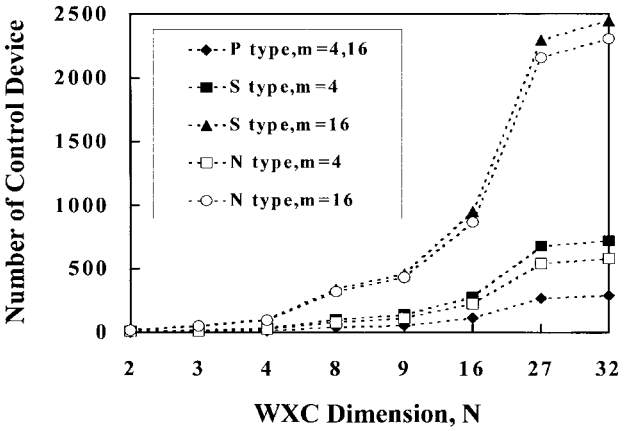


Fig. 10. The number of control devices required for the three FBG-based $N \times N$ WXC's. The parameter, $m$, is the WDM wavelengths per fiber.

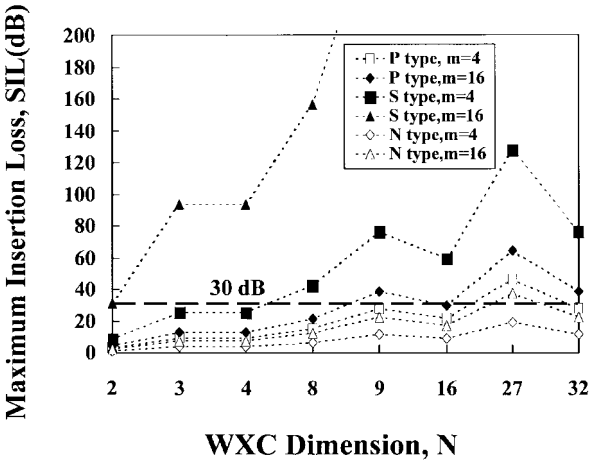


Fig. 11. The maximum (worst-case) system insertion loss for three FBG-based $N \times N$ WXC's. The maximum system attenuation allowed is assumed to be 30 dB.

port 1 to 2 or from port 2 to 3. Typical values for $L_{\rm OC}$ range from 0.4 to 1.0 dB with an isolation of >40 dB. Furthermore, assume that the insertion loss of all $2 \times 2$ and $1 \times K$ OSW's, $L_{\rm SW}$, is about 0.9 dB for $K \leq 256$.

For a single $2 \times 2$ WXC, the maximum (worst) insertion loss, $IL_{\max}$, the minimum (least) insertion loss, $IL_{\min}$, and differential insertion loss, $\Delta IL$, of the propagated optical signals for the $P$-type, $S$-type, and $N$-type $2 \times 2$ WXC's are given below.

*1) $P$-Type WXC:*

$$IL_{\max} = 2(L_{\rm OC} + L_{\rm SW}) + 2(m-1) \cdot L_G \tag{5a}$$
$$IL_{\min} = 2(L_{\rm OC} + L_{\rm SW}) \tag{5b}$$
$$\Delta IL = IL_{\max} - IL_{\min} = 2(m-1) \cdot L_G. \tag{5c}$$

*2) $S$-Type WXC:*

$$IL_{\max} = 2(L_{\rm OC} + m \cdot L_{\rm SW}) + 2(m-1) \cdot L_G \tag{5d}$$
$$IL_{\min} = 2(L_{\rm OC} + L_{\rm SW}) \tag{5e}$$
$$\Delta IL = IL_{\max} - IL_{\min} = 2(m-1) \cdot (L_{\rm SW} + L_G). \tag{5f}$$

*3) $N$-Type WXC:*

$$IL_{\max} = 2L_{\rm OC} + 2(m-1) \cdot L_G \tag{5g}$$
$$IL_{\min} = 2L_{\rm OC} \tag{5h}$$
$$\Delta IL = IL_{\max} - IL_{\min} = 2(m-1) \cdot L_G. \tag{5i}$$

The maximum number of the building block "**W**," $W_H$, propagated by an optical signal in the $N \times N$ WXC's is

$$W_H = 2 \cdot (n-1) + 1, \quad \text{for } N = 2^n \tag{6a}$$
$$W_H = 6 \cdot (n-1) + 3, \quad \text{for } N = 3^n. \tag{6b}$$

Therefore, the maximum (worst case) system insertion loss *SIL* for these three-type $N \times N$ WXC's are obtained by $SIL = IL_{\max} \cdot W_H$, and are given below.

*4) $P$-Type $N \times N$ WXC:*

$$SIL = [2(L_{\rm OC} + L_{\rm SW}) + 2(m-1) \cdot L_G] \cdot [2 \cdot (n-1) + 1], \quad \text{for } N = 2^n \tag{7a}$$
$$SIL = [2(L_{\rm OC} + L_{\rm SW}) + 2(m-1) \cdot L_G] \cdot [6 \cdot (n-1) + 3], \quad \text{for } N = 3^n. \tag{7b}$$

*5) $S$-Type $N \times N$ WXC:*

$$SIL = [2(L_{\rm OC} + m \cdot L_{\rm SW}) + 2(m-1) \cdot L_G] \cdot [2 \cdot (n-1) + 1], \quad \text{for } N = 2^n \tag{7c}$$
$$SIL = [2(L_{\rm OC} + m \cdot L_{\rm SW}) + 2(m-1) \cdot L_G] \cdot [6 \cdot (n-1) + 3], \quad \text{for } N = 3^n. \tag{7d}$$

*6) $N$-Type $N \times N$ WXCL:*

$$SIL = [2L_{\rm OC} + 2(m-1) \cdot L_G] \cdot [2 \cdot (n-1) + 1], \quad \text{for } N = 2^n \tag{7e}$$
$$SIL = [2L_{\rm OC} + 2(m-1) \cdot L_G] \cdot [6 \cdot (n-1) + 3], \quad \text{for } N = 3^n. \tag{7f}$$

The *SIL* for these three-type rearrangeably nonblocking $N \times N$ WXC's is plotted in Fig. 11. Here, the values for the insertion loss of each circulator, OSW, and FBG elements are assumed to be $L_{\rm OC} = 0.5$ dB, $L_{\rm SW} = 0.9$ dB, and $L_G = 0.05$ dB, respectively. For this comparison, the maximum attenuation allowed from system input to output without amplification or regeneration is assumed to be 30 dB. It can be seen from the figure that the $N$-type and $P$-type architectures have significantly better insertion loss characteristics for larger WXC dimensions. The $N$-type WXC has the best system attenuation of 22.5 dB even for $N = 32$ and $m = 16$ because that no OSW's are used in such architecture. The $S$-type architecture has the worst system attenuation due to many cascaded $2 \times 2$ OSW's in such WXC, which is increased drastically for more WDM wavelengths used per fiber. The $P$-type WXC has satisfactory system attenuation for $N \leq 16$ because only a pair of $1 \times K$ OSW used.

Similarly, The minimum number of the building block "**W**," $W_L$, propagated by an optical signal in the $N \times N$ WXC's can also be obtained. Let us have a differential number $W_D \equiv W_H - W_L$, then the $W_D$ of $N \times N$ WXC's is

$$W_D = 0, \quad \text{for } N = 2^n \tag{8a}$$
$$W_D = 2 \cdot (n-1) + 1, \quad \text{for } N = 3^n. \tag{8b}$$

The differential insertion loss, $\Delta SIL$, is the difference between the highest loss path (i.e., the worst case) and the lowest loss

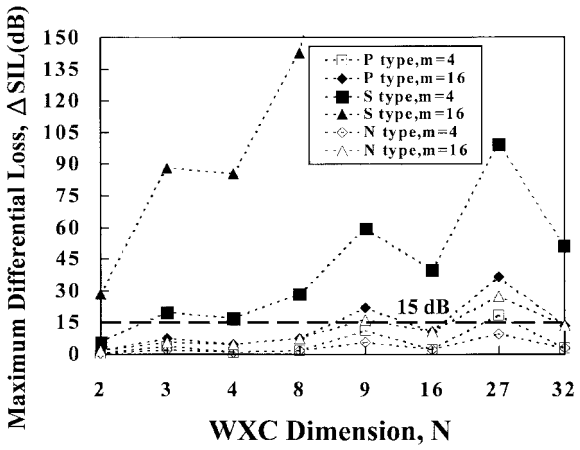


Fig. 12. The maximum (worst-case) differential system insertion loss for three FBG-based $N \times N$ WXC's. The maximum differential loss allowed is assumed to be 15 dB.

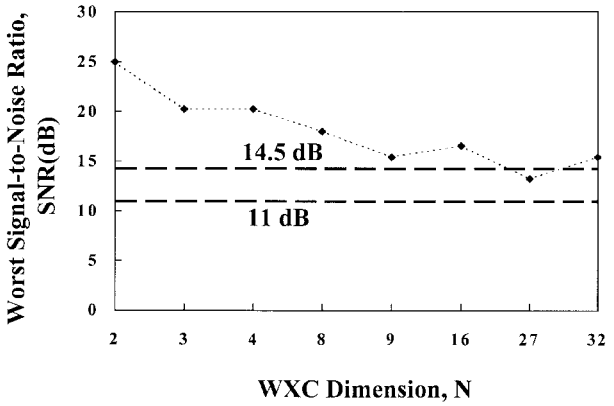


Fig. 13. The worst-case system SNR as a function of WXC dimension. The required SNR to achieve a system BER performance of $1 \times 10^{-9}$ is assumed to be grater than 11 dB and 14.5 dB for the channel rate of 2.5 and 10 Gb/s, respectively.

path, and thus $\Delta SIL = (IL_{\max} \cdot W_H) - (IL_{\min} \cdot W_L) = (\Delta IL \cdot W_H) + (IL_{\min} \cdot W_D)$. Here, $IL_{\max}$, $IL_{\min}$, and $\Delta IL$ are described in (5); the $W_H$ and $W_D$ are described in (6) and (8), respectively. The $\Delta SIL$ for these three-type rearrangeably nonblocking $N \times N$ WXC's is plotted in Fig. 12. For comparison, the maximum differential attenuation allowed for a WXC is assumed to be 15 dB. This differential insertion loss is based on both the capability of the receiver dynamic range at each receiving node, and the input dynamic range capability of the optical limiting amplifier (OLA), to be described in Section V. This differential attenuation loss can be easily compensated by an OLA located at each output fiber of the WXC because an OLA with an input dynamic range of 20–30 dB can be easily reached. The $N$-type WXC has the lowest differential system attenuation of $\leq$13.5 dB for $N = 32$ and $m = 16$ because that no OSW's are used in this architecture. The $S$-type architecture also has the worst differential system insertion loss due to many cascaded series OSW's used in the WXC, which is also increased drastically for more WDM wavelengths per fiber used. The $P$-type WXC has satisfactory differential system attenuation of 10.2 dB for $N = 16$ and $m = 16$.

Although the assumption of component loss values used for system attenuation and differential attenuation comparisons of different FBG-based WXC's seems very low, it is reasonable for most of currently commercial components. On the other hand, it is possible to have low splicing loss between FBG's in the $N$- and $P$-type WXC's by excellent splicing works or by photo-imprinting different FBG's on a same fiber to form the desired FBG chain. Furthermore, the connection loss between the mechanical switch and FBG chain could be less than 0.1 dB, which has been included within the insertion loss of mechanical optical switch. In consequence, with the progress of fabrication technology of various components, the assumption of low component loss values can be realized for most of currently and near-future commercial components.

### *E. SNR Characteristics*

Each FBG element that the signal passes through introduces a small amount of crosstalk between the signal channels with same wavelengths but from different fiber links. The higher the reflectivity, $R$(%), of a given FBG element, the lower the crosstalk will be. The extinction ratio of a single FBG element in dB is defined as $X = |10\log_{10}(1-R)|$. Typical values for $X$ can vary from 10 dB up to 45 dB, depending upon the reflectivity and fabrication characteristics of FBG elements. The SNR for an $N \times N$ WXC can be estimated by determining the number of the building block's "**W**" that the signal channel passes through and how much power will be leaked into the same-wavelength channel at each building block "**W**."

Three assumptions can be reasonably made in the following for derivation of the system per-channel SNR. First, the back-reflection characteristics of all optical components are excellent with return loss of 65 dB. Second, the crosstalk between different channels but with same wavelength is dominated by the first "$W$" building block of the traveled optical path in an $N \times N$ WXC. Third, the crosstalk from other WDM channels in each building block can be neglected. Then, the worst-case per-channel SNR characteristics can be calculated by SNR $= X - 10\log_{10}(W_H)$ for $N \times N$ WXC's in spite of $P$-type, $S$-type or $N$-type architectures, where $W_H$ is the maximum number of the building block that the signal passes through in the WXC's. The SNR characteristics have also been plotted as a function of WXC dimension in Fig. 13. This graph assumes an extinction ratio, $X$, of 25 dB of all FBG's (with reflectivity of 99.7%) for all WXC architectures. The required SNR is assumed to be grater than 11 dB for the channel bit rate of 2.5 Gb/s and to be greater than 14.5 dB for the channel bit rate of 10 Gb/s to achieve a system BER performance of $1 \times 10^{-9}$. From Fig. 13, we find that the rearrangeably nonblocking WXC meeting the SNR requirement for both 2.5 Gb/s and 10 Gb/s channel-rate operations has network dimension $N$ of 32 with $m = 16$.

Because the $\Delta SIL$ is the attenuation difference between the highest loss path (i.e., the worst-case) and the lowest loss path in the WXC, thus the SNR considered here is really the worst case per-channel SNR. Assume all WDM signal channels have same optical power level in the input fiber of WXC. If the worst case per-channel SNR of a WXC is satisfied with the minimum requirement of system SNR, then other signal

TABLE III
THE ESTIMATED DIMENSION LIMITS OF THE $P$-TYPE, $S$-TYPE, AND $N$-TYPE REARRANGEABLY NONBLOCKING WXC ARCHITECTURES, AND THE ASSOCIATED LIMITING FACTORS FOR DIFFERENT NUMBERS OF WDM WAVELENGTHS PER FIBER AT 2.5 OR 10 Gb/s CHANNEL RATES

| WXC Architectures | | Estimated Dimension Limits | | |
|---|---|---|---|---|
| | Wavelengths per fiber, m | 2.5 Gb/s Channel Rates | 10 Gb/s Channel Rates | Notes |
| N-type | m = 4 | 4096 × 4096 (limited by SIL) | 64 × 64 (limited by SNR) | |
| | m = 8 | 512 × 512 (SIL) | 64 × 64 (SIL) | |
| | m =16 | 32 × 32 (ΔSIL) | 32 × 32 (ΔSIL) | 27 × 27 exclusive |
| P-type | m = 4 | 32 × 32 (SIL) | 32 × 32 (SIL) | 27 × 27 exclusive |
| | m = 8 | 16 × 16 (1 × K OSW) | 16 × 16 (1 × K OSW) | 9 × 9 exclusive |
| | m =16 | ✗ | ✗ | |
| S-type | m = 4 | 2 × 2 (ΔSIL) | 2 × 2 (ΔSIL) | |
| | m = 8 | ✗ | ✗ | |
| | m =16 | ✗ | ✗ | |

channels will have more better SNR. Therefore, the differential attenuation effect in the worst case SNR calculation is implied.

## IV. WXC DIMENSION LIMITS

This estimation of WXC dimension limits assumes the following values of $L_{\rm OC} = 0.5$ dB, $L_{\rm SW} = 0.9$ dB, $L_G = 0.05$ dB, and $X = 25$ dB. The maximum acceptable system attenuation of 30 dB, a maximum differential attenuation of 15 dB, and a minimum acceptable system SNR of 11 dB for 2.5 Gb/s and of 14.5 dB for 10 Gb/s channel line rates are also assumed. Furthermore, the return loss characteristic for all optical component and connectors used has excellent quality of about 65 dB. Within these limits, the largest size of the FBG-based WXC's can be estimated. Table III lists the estimated dimension limits of the $P$-type, $S$-type, and $N$-type rearrangeably nonblocking WXC architectures and the associated limiting factors for different numbers of WDM wavelengths per fiber at 2.5 or 10 Gb/s channel rates.

Note that the $N$-type WXC architecture can grow to a 4096 × 4096, 512 × 512, and 32 × 32 dimensions for WXC's employing four, eight, and sixteen WDM wavelengths per fiber, respectively, with 2.5 Gb/s channel rate operations. These WXC sizes are limited due to the unacceptable *SIL*, *SIL*, and Δ*SIL*, respectively. For 10 Gb/s channel-rate operations, the $N$-type WXC architecture can operate to a 64 × 64, 64 × 64, and 32 × 32 dimensions for WXC's employing four, eight, and sixteen WDM wavelengths per fiber, respectively. These WXC sizes are limited due to the unacceptable *SNR*, *SIL*, and Δ*SIL*, respectively, wherein the 27 × 27 WXC is not included for supporting operation of sixteen WDM wavelengths per fiber due to the excess Δ*SIL* and *SIL* characteristics for both 2.5 and 10 Gb/s channel rates.

For the $P$-type WXC architecture, it can only grow to a 32 × 32 and 16 × 16 dimensions for WXC's employing four and eight WDM wavelengths per fiber, respectively, for both 2.5 Gb/s and 10 Gb/s channel-rate operations. These WXC sizes are limited due to the unacceptable *SIL* and the maximum size of 1 × $K$ OSW, respectively. Wherein the 27 × 27 and 9 ×9 WXC is exclusive for supporting operation of four and eight WDM wavelengths per fiber, respectively, due to the excess *SIL* for both 2.5 and 10 Gb/s channel rates. The $P$-type WXC architecture can operate with sixteen WDM wavelengths per fiber in a 16 × 16 WXC size for both 2.5 and 10 Gb/s channel rates only when the low-loss 1 × $K$ OSW with size of $K = 2^8 = 256$ is available. On the contrary, the $S$-type WXC architecture can only operate with four WDM wavelengths per fiber in a 2 × 2 WXC size, due to the unacceptable differential system loss Δ*SIL*, at both 2.5 and 10 Gb/s channel rates. Table IV lists the numbers of required FBG's and optical circulators for each limit case of the $P$-type, $S$-type, and $N$-type rearrangeably nonblocking WXC architectures presented in Table III. For most WDM networks, the WXC dimension $N$ is $\leq$16 with 4–16 WDM channel wavelengths. Therefore, only the $N$-type architecture meets the 2.5- and 10-Gb/s system requirements, and can be constructed by using the least number of required FBG's, control devices, and OC's. As the values for $L_{\rm OC}$, $L_{\rm SW}$, and $L_G$ decrease, or $X$ increases, or the acceptable limits for attenuation, or differential attenuation improve, the obtainable sizes for all of the architectures will increase.

TABLE IV
THE NUMBERS OF REQUIRED FBG'S AND OPTICAL CIRCULATORS FOR EACH LIMIT CASE OF THE $P$-TYPE, $S$-TYPE, AND $N$-TYPE WXC ARCHITECTURES PRESENTED IN TABLE III

| | | 2.5 Gb/s rates | | | 10 Gb/s rates | | |
|---|---|---|---|---|---|---|---|
| WXC | m | Dimension | FBGs | OCs | Dimension | FBGs | OCs |
| N-type | 4 | 4096 × 4096 | 188,416 | 94,208 | 64 × 64 | 1,408 | 704 |
| | 8 | 512 × 512 | 34,816 | 8,704 | 64 × 64 | 2,816 | 704 |
| | 16 | 32 × 32 | 2,304 | 288 | 32 × 32 | 2,304 | 288 |
| P-type | 4 | 32 × 32 | 4,608 | 288 | 32 × 32 | 4,608 | 288 |
| | 8 | 16 × 16 | 57,344 | 112 | 16 × 16 | 57,344 | 112 |
| S-type | 4 | 2 × 2 | 4 | 2 | 2 × 2 | 4 | 2 |

## V. DISCUSSIONS

There are several advantages for these FBG-based WXC's, as compared with other SOA-based or array-waveguide-grating-multiplexer-based WXC's, such as high cross-connect contrast ratio, better interchannel loss uniformity, and potentially low cost. The high cross-connect contrast ratio can be further improved up to >50 dB by employing the ultra-high-reflectivity (∼100%) FBG's, low back-reflection (>65 dB) components, and angled-physical-contact connections in the WXC. The uniformly low interchannel loss is due to the near spectral-loss independence characteristics of the OC's and/or OSW's in the 1.55-$\mu$m band. Because of successful development of FBG's [17] and other optical components, the FBG-based WXC has potentially lower cost, especially for the $N$-type WXC, than other actively space-division-switch-based or wavelength-converter-based WXC's. Furthermore, the simple structure and operation mechanism of FBG-based

TABLE V
COMPARISON BETWEEN THE PROPOSED FBG-BASED WXC AND OTHER OPTICAL WXC'S

| WXC type | Key Technologies | Pros | Cons | Ref. |
|---|---|---|---|---|
| 1.Mux./demux.-based WFXC | • WDM mux./demux. pair | • Simple<br>• Polarization insensitivity | • Rearrangeability<br>• Scalability and Modularity | [1, 3] |
| 2.m-OSW-SD-based WSXC | • Mechanical Optical Switch (m-OSW) + mux./demux. | • Simple<br>• Crosstalk<br>• Polarization insensitivity | • Bulky<br>• Scalability and Modularity | [32] |
| 3.SOA-SD-based WSXC | • SOAs + mux./demux. | • Switching speed ($\mu$s) | • Polarization sensitivity<br>• Crosstalk | [5, 7] |
| 4.Wavelength-converter-based WIXC | • Cross-gain/cross-phase SOAs + SD + mux./demux. | • Strictly nonblocking<br>• Modularity | • Complexity<br>• Integration required | [4, 22, 33] |
| 5.Optoelectronic-conversion-based WSXC | • Optical transmitters /receivers + demux. + optical combiner | • Optical power and SNR | • Bit-rate and format inflexibility | [34] |
| 6.PAWG-based WSXC | • PAWG + thermal Optical (TO) switch array | • Integrated and compact | • Loss and uniformity<br>• Crosstalk and port dimensions | [9, 35] |
| 7.FBG-based WSXC | • FBGs + m-OSWs/ controls + OCs | • Crosstalk<br>• Loss and uniformity<br>• Capacity expansion<br>• Cost (potentially) | • Bulky<br>• Modularity | This work |

WXC's make them to be easily expanded to a greater number of WDM channels per fiber. This can be achieved by adding desired FBG chains between the OSW pair (for $P$-type) or by splicing desired FBG elements in the FBG chain (for $N$-type). The wavelength contention problem for the WDM networks using FBG-based wavelength-routed WXC's can be avoided by proper global allocation of paths and associated transport resources (fiber and wavelength). Thus, capacity expansion of the FBG-based WXC can be easily realized, however, expansion of more input/output ports (i.e., modularity) is difficult, thus reinterconnecting WXC subnetworks is unavoidable. The comparison between the FBG-based and other optical WXC's is shown in Table V, in which the acronyms of WFXC, WSXC, and WIXC represent the wavelength *fixed*, *selective*, and *interchangeable* cross-connects, respectively. The PAWG and SD stand for the phase array waveguide grating and the space division switch fabric, respectively.

The question of wavelength channel spacing is an important issue in long-haul WDM transmission systems [24], [25] and WXC networks [4]. When wavelength channel are equally spaced, the product terms generated by four-wave mixing (FWM) between channels fall exactly at the channel wavelengths and hence cause crosstalk [24], [25]. This is particular severe when dispersion-shifted fiber are used. An effective technique to circumvent the FWM crosstalk is to use unequal channel spacing so that the FWM waves do not coincide with the channel wavelengths [24], [25]. For this reason, it is necessary to use unequally spaced wavelength channels in WXC's rather than to use equally spaced wavelength channels [4]. Fortunately, the design of an FBG-based WXC with unequally spaced channels is the same as that of a WXC with equally spaced channels only by placing the desired high-reflectivity FBG elements with proper central wavelengths, which matches the unequally spaced WDM channel wavelengths.

Multiwavelength amplification is required at least on the transmission links and at the interfaces with the WXC's to compensate for the transmission loss and WXC insertion losses. Silica-based EDFA's suffer from limitations in multi-channel operation due to their highly wavelength dependent gain profile in the 1530–1560 nm window. Proper power and/or gain equalization [26]–[28] of silica-based EDFA's should be implemented to cover the full 30-nm amplification region. On the other hand, the fluoride-based EDFA's [29] that exhibit without equalization a gain excursion of 1.5 dB in the 1530–1560 nm region can be an alternative for multiwavelength amplification. However, the differential insertion loss introduced by the WXC cannot be eliminated through these gain-equalized silica-based or fluoride-based EDFA's. An effective way not only to avoid equalization techniques but also to compensate the system attenuation and simultaneously to eliminate the system differential insertion loss introduced by the WXC is to employ multiwavelength optical limiting amplifiers (OLA's) [30], [31]. The chirped-FBG-based OLA [31] configuration, consisting of a three-port optical circulator followed by a bidirectional EDFA (without built-in optical isolators) along with multiple cascaded chirped FBG's will be the most promising candidate to be used. Each high-reflectivity chirped FBG, with appropriate dispersion compensating capability to compensate the preceding fiber link, has a central wavelength corresponding to the unequally spaced WDM channel wavelengths. The OLA's used at each output port of the WXC not only may offer power-limiting operation with high constant channel output power for a large input-signal range from $-35$ to 0 dBm, but also can provide dispersion compensation, especially attractive for the 10 Gb/s networks.

## VI. CONCLUSION

We have proposed and discussed three FBG-based $P$-, $S$-, and $N$-type building blocks with optical circulators and related control devices for constructing $N \times N$ WXC's. Large rearrangeably nonblocking WXC structures based on a three-stage Clos network using these building blocks have been constructed and investigated. Based on reasonable performance assumptions, we have estimated that the system dimensions of $N$-, $P$-, and $S$-type WXC's can grow to a $32 \times 32$, $16 \times 16$, and $2 \times 2$ sizes, respectively, for both 2.5 Gb/s and 10 Gb/s WDM channel operations. The number of WDM wavelengths used per fiber for this $N$-type WXC is sixteen. The fewer WDM wavelengths used per fiber, the larger WXC dimension can be realized. However, the number of WDM wavelengths used per fiber is limited by $m \leq 8$ and $m \leq 4$ for $P$-type and $S$-type WXC's, respectively, due to the commercial $1 \times 256$ OSW and the unacceptable differential system loss, respectively.

The system capacity expansion of the FBG-based WXC can be easily realized by adding new FBG chains between the OSW pair (for $P$-type) or by splicing new FBG elements in the FBG chain (for $N$-type), however, with low modularity. On the other hand, the design of FBG-based WXC can fit operations of unequally spaced channels to circumvent the FWM crosstalk, especially in low dispersion fiber networks. Furthermore, utilization of chirped FBG-based multiwavelength optical limiting amplifiers without any additional equalization techniques seem to be an effective way, besides compensating

the dispersion of the preceding fiber link, to simultaneously compensate system loss and eliminate differential insertion loss introduced by the WXC.

## ACKNOWLEDGMENT

The authors appreciate the useful discussions with S. K. Liaw, and would like to thank C. H. Chang and J. H. Su for drawing the illustrations.

## REFERENCES

[1] Special Issue on Multi-wavelength Optical Technology and Networks, *J. Lightwave Technol.*, vol. 14, June 1996.
[2] Special Issue on System and Network Applications of Optical Amplifiers, *J. Lightwave Technol.*, vol. 13, May 1995.
[3] C. A. Brackett, "Forward—Is there an emerging consensus on WDM networking?," *J. Lightwave Technol.*, vol. 14, pp. 936–941, June 1996.
[4] W. D. Zhong, J. P. R. Lacey, and R. S. Tucker, "Multiwavelength cross-connects for optical transport networks," *J. Lightwave Technol.*, vol. 14, pp. 1613–1620, July 1996.
[5] Y. Jin and M. Kavehrad, "An optical cross-connect system as high-speed switching core and its performance analysis," *J. Lightwave Technol.*, vol. 14, pp. 1183–1197, June 1996.
[6] R. A. Spanke, "Architectures for guided-wave optical space switching systems," *IEEE Commun. Mag.*, vol. 25, pp. 42–48, 1987.
[7] R. F. Kalman, L. G. Kazovsky, and J. W. Goodman, "Space division switches based on semiconductor optical amplifiers," *IEEE Photon. Technol. Lett.*, vol. 14, pp. 1048–1051, 1992.
[8] Y. K. Chen and W. I. Way, "Multiwavelength line-rate-independent optical digital cross-connects based on low-gain fiber amplifiers," *IEEE Photon. Technol. Lett.*, vol. 6, pp. 1122–1125, 1994.
[9] O. Ishida, H. Takahashi, S. Suzuki, and Y. Inoue, "Multichannel frequency-selective switch employing an array-waveguide grating multiplexer with fold-back optical paths," *IEEE Photon. Technol. Lett.*, vol. 6, pp. 1219–1221, 1994.
[10] T. Durhuus, B. Mikkelsen, C. Joergensen, S. L. Danielsen, and K. E. Stubkjaer, "All-optical wavelength conversion by semiconductor optical amplifiers," *J. Lightwave Technol.*, vol. 14, pp. 942–954, 1996.
[11] S. J. B. Yoo, "Wavelength conversion technologies for WDM network applications," *J. Lightwave Technol.*, vol. 14, pp. 955–966, 1996.
[12] C. Clos, "A study of nonblocking switching networks," *Bell Syst. Tech. J.*, pp. 407–425, Mar. 1953.
[13] V. E. Benes, "On rearrangeable three-stage connecting networks," *Bell Syst. Tech. J.*, pp. 1481–1492, Sept. 1962.
[14] K. O. Hill, Y. Fujii, D. C. Johnson, and B. S. Kawasaki, "Photosensitivity in optical fiber waveguides: Application to reflection filter fabrication," *Appl. Phys. Lett.*, vol. 32, pp. 647–649, 1978.
[15] G. Meltz, W. W. Morey, and W. H. Glenn, "Formation of Bragg gratings in optical fibers by a transverse holographic method," *Opt. Lett.*, vol. 14, pp. 823–825, 1989.
[16] C. R. Giles, "Lightwave applications of fiber Bragg gratings," *J. Lightwave Technol.*, vol. 15, pp. 1391–1404, Aug. 1997.
[17] Special Issue on Fiber Gratings, Photosensitivity, and Poling, *J. Lightwave Technol.*, vol. 15, Aug. 1997.
[18] H. Okayama, Y. Ozeki, T. Kamijoh, C. Q. Xu, and I. Asabayashi, "Dynamic wavelength selective add/drop node comprising fiber grating and optical switches," *Electron. Lett.*, vol. 33, pp. 403–404, 1997.
[19] A. D. Ellis, R. Kashyap, I. Crisp, and D. J. Malyon, "Dispersion compensating, reconfigurable optical add drop multiplexer using chirped fiber Bragg gratings," *Electron. Lett.*, vol. 33, pp. 1474–1475, 1997.
[20] Y. K. Chen, S. K. Liaw, and C. C. Lee, "Dynamically selective multiwavelength cross-connect based on fiber Bragg gratings and optical switches," *Opt. and Quantum Electron.*, vol. 30, pp. 121–127, 1998.
[21] G. A. Ball and W. W. Morey, "Compression-tuned single-frequency Bragg grating fiber laser," *Opt. Lett.*, vol. 19, pp. 1979–1981, 1994.
[22] A. Jourdan, F. Masetti, M. Garnot, G. Soulage, and M. Sotom, "Design and implementation of a fully reconfigurable all-optical crossconnect for high capacity multiwavelength transport networks," *J. Lightwave Technol.*, vol. 14, pp. 1198–1206, June 1996.
[23] M. Koga, Y. Hamazumi, A. Watanabe, S. Okamoto, H. Obara, K. I. Sato, M. Okuno, and S. Suzuki, "Design and performance of an optical path cross-connect system based on wavelength path concept," *J. Lightwave Technol.*, vol. 14, pp. 1106–1119, June 1996.
[24] F. Forghieri, R. Tkach, and A. R. Chraplyvy, "Reduction of four-wave mixing cross-talk in the WDM systems using unequally spaced channels," *IEEE Photon. Technol. Lett.*, vol. 6, pp. 754–756, 1994.
[25] R. W. Tkach, A. R. Chraplyvy, F. Forghieri, A. H. Gnauck, and R. M. Derosier, "Four-photon mixing and high-speed WDM systems," *J. Lightwave Technol.*, vol. 13, pp. 841–849, May 1995.
[26] A. R. Chraplyvy, J. A. Nagel, and R. W. Tkach, "Equalization in amplified WDM lightwave transmission systems," *IEEE Photon. Technol. Lett.*, vol. 4, pp. 920–922, 1992.
[27] I. Eskildsen, E. Goldstein, V. da Silva, M. Andrefco, and Y. Silberberg, "Optical power equalization for multiwavelength fiber-amplifier cascades using periodic inhomogeneous broadening," *IEEE Photon. Technol. Lett.*, vol. 5, pp. 1118–1190, 1993.
[28] Y. K. Chen and S. K. Liaw, "Optimum gain-equalised configuration of widwband erbium-doped fiber amplifier using inter-stage samarium-doped fiber and midway isolator," *Electron. Lett.*, vol. 32, no. 23, pp. 2175–2177, Nov. 1996.
[29] D. Bayart, J. Hervo, and F. Chiquet, "Impact of fluoride-based EDFA's gain flatness on design of WDM amplifier cascade," in *Tech. Dig. Opt. Fiber Commun. (OFC'95)*, San Diego, CA, paper TuP2, 1995.
[30] Y. K. Chen, S. K. Liaw, W. Y. Guo, and S. Chi, "Multiwavelength erbium-doped power limiting amplifier in all-optical self-healing ring network," *IEEE Photon. Technol. Lett.*, vol. 8, pp. 842–844, 1996.
[31] S. K. Liaw, C. C. Lee, Y. K. Chen, K. P. Ho, and S. Chi, "Chirped-fiber-grating-integrated optical limiting amplifier for dispersion compensation," in *Tech. Dig. IEEE/Laser and Electro-Optics Soc. Annu. Meeting (LEOS'97)*, paper MC3, Nov. 1997.
[32] N. V. Srinivasan, "Add-drop multiplexers and cross-connects for multiwavelength optical networking," in *Tech. Dig. Opt. Fiber Commun. (OFC'98)*, San Jose, CA, paper TuJ1, 1998.
[33] M. Berger, M. Chbat, A. Jourdan, M. Sotom, P. Demeester, B. V. Caenegem, P. Godsvang, M. Huber, R. Marz, A. Leclert, T. Olsen, G. Tobolka, and T. V. den Broeck, "Pan-European optical networking using wavelength division multiplexing," *IEEE Commun. Mag.*, pp. 82–88, Apr. 1997.
[34] Y. Hamazumi, M. Koga, M. Ishii, S. Suzuki, and K. Sato, "Transport performance in optical path cross-connect system employing unequally spaced channel allocation," *J. Lightwave Technol.*, vol. 15, pp. 616–627, Apr. 1997.
[35] H. Li, C. H. Lee, S. Zhong, Y. J. Chen, M. Dagenais, and D. Stone, "Multiwavelength integrated $2 \times 2$ optical cross-connect switch and lambda-partitioner with $2 \times N$ phase-array waveguide grating in self-loopback configuration," in *Tech. Dig. Opt. Fiber Commun. (OFC'98)*, San Jose, CA, paper TuN4, 1998.

**Yung-Kuang Chen** (M'97) was born in 1960. He received the M.Sc. and the Ph.D. degrees in electrooptical engineering from the National Central University, Taiwan, in 1987 and the National Chiao-Tung University, Taiwan, in 1995, respectively.

In 1988, he joined the Telecommunication Laboratories, Ministry of Transportation and Communications, Taiwan. Since then, he has been working on subsystem and system technologies of optical fiber communications, including wavelength division multiplex (WDM) transmission and erbium-doped fiber amplifiers (EDFA's). After research experience at Telecommunication Laboratories for seven years, he became an Associate Professor at the Institute of Electro-Optical Engineering, National Sun Yat-Sen University, Taiwan, in August 1995. His current research interests include EDFA applications for WDM transmission and fiber-optic sensing systems, applications of fiber Bragg gratings for WDM networks, analog video hybrid fiber-coaxial (HFC) networks and associated in-service surveillance technologies.

Dr. Chen is the member of the IEEE Lasers and Electro-Optics Society (LEOS) and the Optical Society of America (OSA).

**Chien-Chung Lee** was born in 1964. He received the M.Sc. degree in electrooptical engineering from National Central University, Taiwan, in 1991. He is currently working towards the Ph.D. degree.

In 1991, he joined the Telecommunication Laboratories, Ministry of Transportation and Communications, Taiwan (now renamed as Chung-Hwa Telecommunication Laboratories) Since then, he has been working on fiber-in-the-loop (FITL) technologies, including fiber measurement and optical CATV transmission. His current research interests include in-service surveillance technologies for optical networks, and applications of EDFA for WDM transmission and analog video HFC networks.